cells by the same treatment (Figs. 1*A* and 4), suggesting that the LA treatment works exclusively for the internalization of insoluble α-syn aggregates.

These results strongly suggest that α-syn fibrils are incorporated with the aid of LA but do not exclude the possibility that extracellular α-syn fibrils may induce aggregation of endogenous α-syn without incorporation. To confirm that the extracellular α-syn fibril seeds are internalized into cells by LA, we performed the transduction of preformed carboxyl-terminally HA-tagged α-syn fibril seeds (Seed-HA) instead of non-tagged

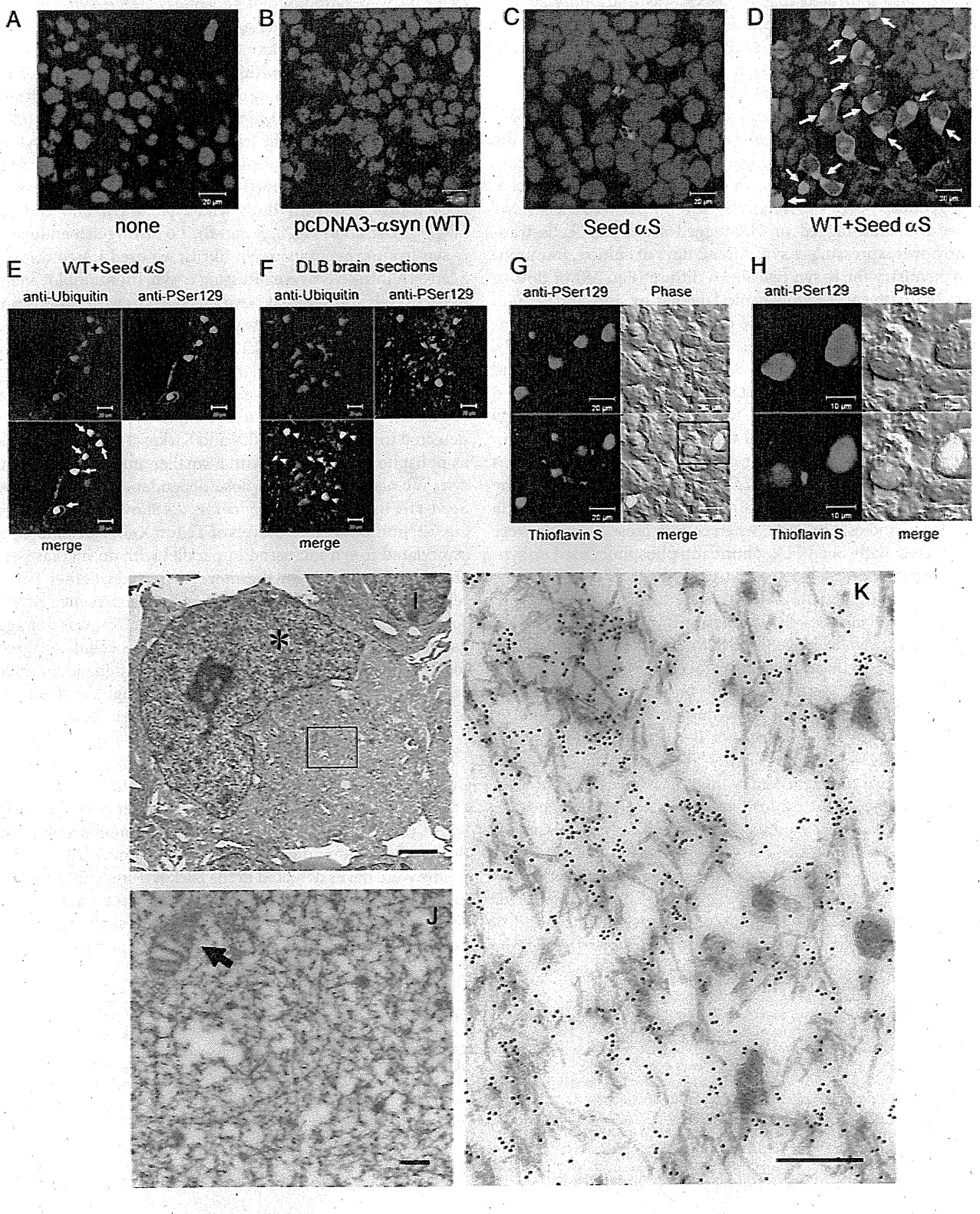

α-syn seeds. As shown in Fig. 1, *B* and *C*, time course experiments revealed that Seed-HA was also incorporated into cells in the presence of LA and could be detected with both anti-HA antibody and a phospho-α-syn-specific antibody (anti-Ser(P)^{129}), even 3 days after infection. Confocal microscopic analyses also indicated that Seed-HA was phosphorylated at Ser^{129} intracellularly. All anti-Ser(P)^{129}-positive dotlike structures were also stained with anti-HA, indicating that no endogenously phosphorylated α-syn aggregates are present in the cells (Fig. 1*D* and supplemental Fig. S1*C*).

Establishment of a Cell Culture Model for Nucleation-dependent Polymerization of α-Syn—Although introduction of the seed α-syn into cells was accompanied with phosphorylation, no further dramatic change was observed. Because the level of endogenous α-syn was relatively low in SH-SY5Y cells, we introduced non-tagged or HA-tagged seeds into cells transiently overexpressing α-syn. After 3 days of culture, immunocytochemistry for α-syn revealed a diffuse (Fig. 2*B*) or dotlike (Fig. 2*C*) pattern of cytoplasmic labeling by anti-Ser(P)^{129} in cells transfected with wild-type α-syn without seeds or in non-overexpressing cells with Seed αS, respectively. Surprisingly, however, in cells transfected with both pcDNA3-α-syn and Seed αS, we observed abundant round inclusions that occupied the cytoplasm and displaced the nucleus, with morphology highly reminiscent of cortical-type Lewy bodies observed in human brain (Fig. 2*D*). The size of the α-syn-positive inclusions was ~10 μm in diameter (Fig. 2*D*), which is similar to that of the Lewy bodies detected in the brains of patients with dementia with Lewy bodies. Similarly, when cells expressing α-syn were transfected with Seed-HA, abundant phosphorylated α-syn-positive cells were also detected (supplemental Fig. S1*D*).

We next examined the status of ubiquitin, which is positive in most types of intracellular filamentous inclusions, including Lewy bodies, in neurodegenerative disease brains. As shown in Fig. 2*E*, we found that almost all intracellular inclusions labeled with anti-Ser(P)^{129} were also positive for ubiquitin, as is the case for Lewy bodies in the cortex of human DLB brain (Fig. 2*F*). Furthermore, the juxtanuclear Ser(P)^{129}-positive, Lewy body-like inclusions were also positively labeled with thioflavin S, a fluorescent dye that specifically intercalates within structures rich in β-pleated sheet conformation (Fig. 2, *G* and *H*), indicating that the inclusions contain β-sheet-rich filamentous aggregates. Electron microscopic analysis of cells transfected with both wild-type α-syn and the seeds revealed that the inclusions are composed of filamentous structures ~10 nm in diameter that are often covered with granular materials (Fig. 2, *I* and *J*). The filamentous structures were randomly oriented within the cytoplasm of these cells, forming a meshwork-like profile, and were frequently intermingled with mitochondria (Fig. 2, *I* and *J*), being highly reminiscent of human cortical Lewy bodies. Immunoelectron microscopy showed that the filaments were densely decorated with anti-Ser(P)^{129} (Fig. 2*K*), demonstrating that they were composed of phosphorylated α-syn.

To biochemically validate this cellular model and to investigate further the molecular mechanisms underlying nucleation-dependent aggregation within cells, we differentially extracted α-syn from these cells using detergents of various strengths and analyzed the extracts by immunoblotting with anti-Syn102 and -Ser(P)^{129} antibodies. The levels of α-syn in the Sarkosyl-soluble and -insoluble fractions (total α-syn and α-syn phosphorylated at Ser^{129}, respectively) were dramatically increased in cells transfected with both wild-type α-syn and the seeds (*WT + Seed αS* in Fig. 3, *A* and *B*). To distinguish endogenous α-syn from exogenous α-syn fibrils, we used LA to transduce Seed-HA into cells overexpressing α-syn. Immunoblot analyses of these cells showed that HA-tagged α-syn with slower mobility than non-tagged α-syn was detected in the Sarkosyl-insoluble pellets as phosphorylated forms by anti-HA and anti-Ser(P)^{129} antibodies in cells treated with Seed-HA + LA (Fig. 3, *C–E*). Interestingly, in cells expressing α-syn (WT) treated with Seed-HA + LA, much more abundant non-tagged α-syn was detected in the Triton X-100- and Sarkosyl-insoluble fractions as phosphorylated forms with a smaller amount of the HA-α-syn. We also performed a dose dependence experiment with Seed-HA in cells expressing α-syn. As shown in supplemental Fig. S2, immunoreactive levels of Triton X-100-insoluble phosphorylated α-syn increased in parallel with an increase in the amount of Seed-HA. Furthermore, we tested whether Tau protein forms intracellular aggregates in the presence of α-syn seeds instead of Tau seeds. We found that Tau was not aggregated with Seed-HA, confirming that intracellular aggregate formation of soluble α-syn is specific to and dependent on fibril seeds of the same protein (supplemental Fig. S3). This nucleation-dependent polymerization of α-syn in cells was greater at 3 days than at 1 day after transduction of the seeds (Fig. 3*F*).

Negative stain electron microscopic observation of Sarkosyl-insoluble fractions of the cells harboring inclusions revealed anti-Syn102 and Ser(P)^{129}-positive filaments of ~5–10-nm width (Fig. 3, *G* and *H*) that are highly reminiscent of those derived from human α-synucleinopathy brains (21). Such filaments were never detected in the Sarkosyl-insoluble fraction of cells solely overexpressing α-syn (data not shown). These results indicated that the biochemical characteristics of α-syn accumulated in cells forming the Lewy body-like inclusions

FIGURE 2. **Confocal laser and electron microscopic analyses of α-syn inclusions in plasmid-derived α-syn-expressing cells treated with seed α-syn.** *A–D*, confocal laser microscopic analyses of control SH-SY5Y cells transfected with pcDNA3 vector and Lipofectamine alone (*A*), cells transfected with pcDNA3-α-syn (*WT*) (*B*), cells transduced with the seed α-syn (*Seed αS*) (*C*), and cells transfected with both pcDNA3-α-syn and Seed αS (*WT + Seed αS*) (*D*), immunostained with anti-Ser(P)^{129} (*green*), and counterstained with TO-PRO-3 (*blue*). The *arrows* indicate cytoplasmic round inclusions stained with anti-Ser(P)^{129} (*PSer129*). *Scale bars*, 20 μm. *E–F*, comparison of confocal images of cells transfected with both α-syn plasmid and Seed αS (*E*) and tissue sections from DLB brains (*F*) using anti-Ser(P)^{129} (*green*) and anti-ubiquitin antibodies (*red*). Cytoplasmic inclusions in transfected cells (*arrows*) are positive for ubiquitin, like Lewy bodies (*arrowheads*) in DLB brains. *Scale bars*, 20 μm. *G* and *H*, confocal microscopic images of cells transfected with both pcDNA3-α-syn and Seed αS. Cells were stained with 0.05% Thioflavin S (*green*) and anti-Ser(P)^{129} antibody (*red*). The *boxed area* on the *left* is shown in the *right panel*. *Scale bars*, 20 μm on the *left* and 10 μm on the *right*. *I* and *J*, electron microscopic analyses of cells transfected with both pcDNA3-α-syn and Seed αS. High magnification of the boxed area in *I* is shown in *J*. An *asterisk* or *arrow* indicates a nucleus or mitochondrion, respectively. *Scale bars*, 2 μm in *I* and 200 nm in *J*. *K*, immunoelectron microscopic observation of cells transfected with both pcDNA3-α-syn and Seed αS using a polyclonal antibody against phosphorylated Ser^{129} of α-syn. *Scale bar*, 200 nm.

were very similar to those of α-syn deposited in the brains of patients with α-synucleinopathies, including PD and DLB.

Because the idea has been gaining ground that transient oligomers, rather than mature fibrils, are responsible for cytotoxicity, we examined whether soluble oligomers could be introduced into cells in the same manner as fibril seeds by means of LA treatment and whether they could function as seeds for intracellular α-syn aggregate formation. As shown in Fig. 4, *A* and *B*, we purified stable α-syn oligomers from recombinant α-syn treated with exifone, an inhibitor of *in vitro* α-syn aggregation, which is thought to inhibit filament formation of α-syn by stabilizing SDS-resistant soluble oligomers (22, 23). Then cells expressing α-syn or mock plasmid were treated with a mixture of the oligomer fraction (5 μg) and LA and incubated for 3 days. Immunoblot analyses of lysates of these cells did not detect any SDS-resistant soluble oligomeric α-syn, and the levels of phosphorylated α-syn in the Sarkosyl-soluble and -insoluble fractions showed no increase (Fig. 4, *C* and *D*). On the other hand, we observed phosphorylated and deposited α-syn in the Sarkosyl-soluble and -insoluble fractions in cells expressing α-syn treated with Seed αS (Fig. 4, *C* and *D*). These results showed that SDS-resistant soluble oligomer of α-syn could not be introduced into cultured cells in the same manner as monomeric α-syn and/or could not function as seeds for intracellular α-syn aggregation.

Mutagenic Analysis of Nucleation-dependent Assembly of α-Syn—To investigate further the nucleation-dependent polymerization of α-syn, we analyzed the polymerization of α-syn mutated or truncated at various residues or subdomains that are believed to be crucial for its aggregation. Overexpression of A53T familial Parkinson mutant α-syn, which is readily fibrillogenic *in vitro*, in the presence of Seed αS moderately increased the accumulation and phosphorylation of α-syn in the Sarkosyl-soluble and insolu-

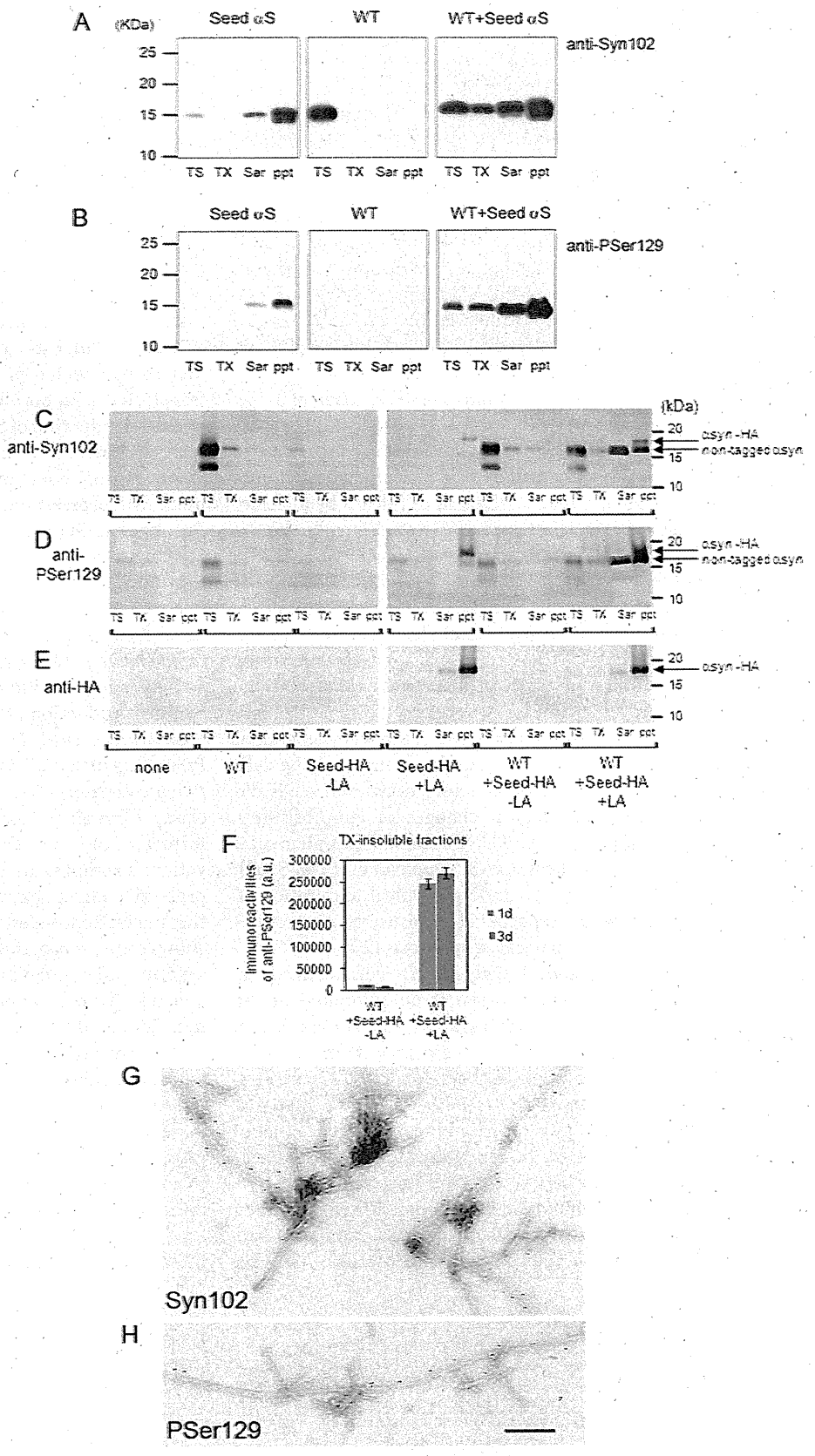

ble fractions compared with those in cells with wild-type α-syn expression and Seed αS (Fig. 5, *A* and *B*). In contrast, overexpression of Δ11 mutant α-syn, an assembly-incompetent mutant lacking residues 73–83, which have been shown to be essential for fibril formation of α-syn (24), elicited neither deposition nor phosphorylation of α-syn. We next introduced α-syn into SH-SY5Y cells expressing S129A mutant α-syn and observed slightly lower levels of Sarkosyl-insoluble α-syn compared with those in cells with wild-type α-syn expression and Seed αS. However, the frequency of inclusion bodies observed in seed-transduced cells expressing S129A was similar to that in seed-transfected cells expressing wild-type α-syn (data not shown), suggesting that phosphorylation at Ser^{129} is not required for the nucleation-dependent polymerization of α-syn within cells.

Nucleation-dependent Intracellular Polymerization of α-Syn Elicits Neurotoxicity and Cell Death—SH-SY5Y cells overexpressing α-syn started to show marked clumping suggestive of cellular degeneration and death by ~48 h after introduction of seeds (Fig. 6*B*). Quantitative analysis of cell death by a lactate dehydrogenase (LDH) release assay at 72 h after introduction of Seed αS showed that cells overexpressing wild-type, A30P, A53T, or S129A α-syn released ~30% of total LDH from total cell lysate, whereas only ~12% of LDH was released from cells expressing Δ11 mutant α-syn, which lacks polymerization ability. In control cells transfected with empty vector or pcDNA3-α-syn followed by treatment with Lipofectamine without seeds, only ~7% of LDH was released (Fig. 6*C*). These results suggest a close correlation between the seed-dependent aggregation of α-syn and cell death. However, the dying cells transfected with fibrillization-competent α-syn and seeds did not show typical morphological changes of apoptosis (*e.g.* nuclear fragmentation, positive TUNEL staining (supplemental Fig. S4*A*), or activation of caspase-3 (supplemental Fig. S4*B*)), suggesting that they did not undergo typical apoptotic cell death, despite a previous report that exposure to neuron-derived extracellular α-syn may cause apoptosis (25).

Impairment of Proteasome Activity in Cells with Intracellular Aggregates of α-Syn—Because α-syn is ubiquitinated in the brains of patients with α-synucleinopathies (26) and inhibition of ubiquitin-proteasome systems by aggregates of proteins with expanded polyglutamine tracts has been reported (27), we analyzed the ubiquitination state of cellular proteins in α-syn aggregate-forming cells and compared the pattern with that in cells treated with a proteasome inhibitor, MG132. A Sarkosyl-soluble fraction of seed-transduced cells expressing wild-type α-syn and harboring abundant inclusions showed increased levels of ubiquitin-positive staining, which was similar in pattern to that observed in cells treated with MG132 (Fig. 6*D*). Because this pattern suggested an impairment of the ubiquitin-proteasome system, we directly analyzed the proteasome activity of α-syn inclusion-forming cells using a specific fluorescent peptide substrate, benzyloxycarbonyl-Leu-Leu-Glu-7-amido-4-methylcoumarin, that emits fluorescence following proteasomal digestion and confirmed that proteasome activity was significantly reduced in these cells as well as in cells treated with 20 μM MG132 for 4 h (Fig. 6*E*). We further examined the suppression of proteasome activity using CL1, a short degron that has been reported to be an effective proteasome degradation signal (28) and whose fusion protein with green fluorescent protein (GFP-CL1) has been used as a reporter for inhibition of proteasomal activity by intracellular polyglutamine aggregates (27) and intracellular α-syn (19). To examine if intracellular α-syn inclusions affected proteasomal activity, SH-SY5Y cells were transfected with both wild-type α-syn and GFP-CL1, followed by the introduction of Seed αS. Fluorescent signals of GFP were scarcely detected in control cells transfected with GFP-CL1 alone (Fig. 6*F*, *none*) but were markedly increased upon treatment with proteasome inhibitor MG132 (Fig. 6*F*, *MG132*), confirming that GFP-CL1 was effectively degraded by proteasome. Strikingly elevated GFP signals were detected in cells forming α-syn inclusions (Fig. 6*F*, *WT + Seed αS*) compared with those in control cells (Fig. 6*F*, *none* or *WT*), and GFP-CL1 and deposits of phosphorylated α-syn were co-localized within these cells (*arrowheads*). These results strongly suggest that proteasome activity is impaired in cells harboring α-syn inclusions elicited by the introduction of Seed αS.

Small Molecular Inhibitors of Amyloid Filament Formation Protect against Cell Death Induced by Seed-dependent α-Syn Polymerization—We have previously shown that several classes of small molecular compounds inhibit amyloid filament formation of α-syn, Tau, and Aβ *in vitro* (17, 23). These observations prompted us to test whether these inhibitors exert a protective effect against death of SH-SY5Y cells mediated by the nucleation-dependent polymerization of α-syn. Fig. 7*A* shows the effects of three polyphenol compounds, exifone, gossypetin, and quercetin, and a rifamycin compound, rifampicin, added to the culture media at a final concentration of 20 or 60 μM. Remarkably, all of these compounds blocked cell death, with gossypetin being the most effective. Our previous *in vitro* studies elucidated that several polyphenols, including gossypetin and exifone, inhibit α-syn assembly and that SDS-stable, noncytotoxic soluble α-syn oligomers are formed in their presence (23), suggesting that such polyphenols may inhibit filament formation of α-syn by stabilizing soluble, prefibrillar intermediates. Gossypetin or exifone might suppress intracellular α-syn aggregate formation by stabilizing such soluble intermediates in cultured cells as well. Immunoblot analysis

FIGURE 3. **Immunoblot and immunoelectron microscopic analyses of intracellular α-syn aggregates in cultured cells.** *A* and *B*, immunoblot analysis of α-syn in cells treated with Seed αS alone (*Seed αS*), pcDNA3-α-syn alone (*WT*), or both WT and Seed αS (*WT + Seed αS*). Proteins were differentially extracted from the cells with Tris-HCl (*TS*), Triton X-100 (*TX*), and Sarkosyl (*Sar*), leaving the pellet (*ppt*). Blots were probed using anti-α-syn (Syn102) (*A*) and anti-$Ser(P)^{129}$ (*PSer129*) (*B*). *C–F*, immunoblot analysis of proteins differentially extracted from mock (none) or cells transfected with pcDNA3-α-syn (*WT*), cells transduced with Seed-HA with (*Seed-HA + LA*) or without LA treatment (*Seed-HA − LA*), and cells overexpressing α-syn treated with Seed-HA with (*WT + Seed-HA + LA*) or without LA treatment (*WT + Seed-HA − LA*). Immunoreactivity of phosphorylated α-syn in the Triton X-100-insoluble fraction was quantified using anti-$Ser(P)^{129}$, and the results are expressed as means ± S.E. ($n = 3$), as shown in *F*. a.u., arbitrary unit. *G* and *H*, immunoelectron microscopy of α-syn filaments extracted from transfected cells. SH-SY5Y cells were transfected with both pcDNA3-α-syn and Seed αS. Sarkosyl-insoluble fraction was prepared from the cells, and the filaments were immunolabeled with anti-Syn102 (*G*) or $Ser(P)^{129}$ (*H*) antibody. *Scale bar*, 200 nm. *1d* and *3d*, 1 and 3 days, respectively.

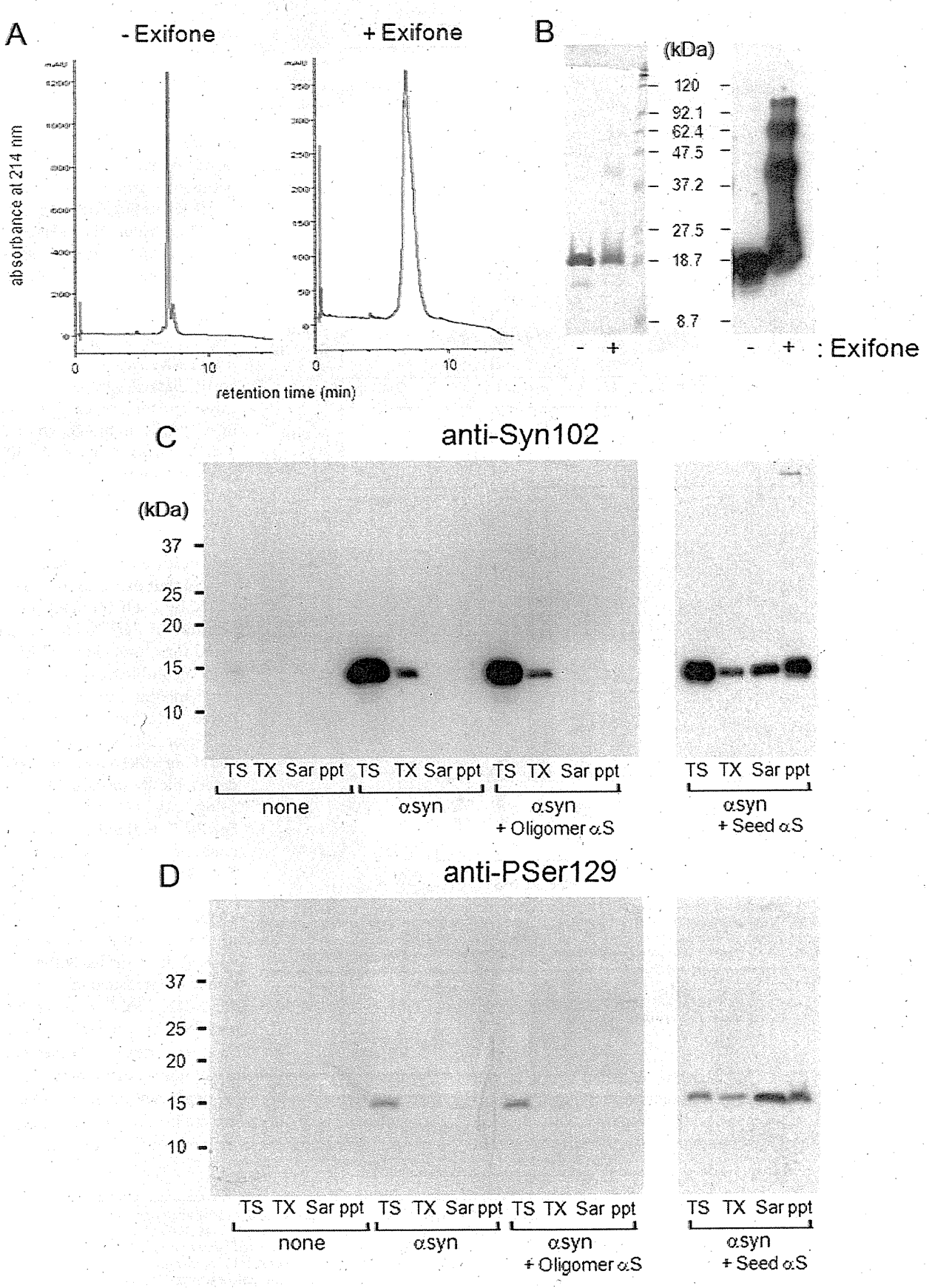

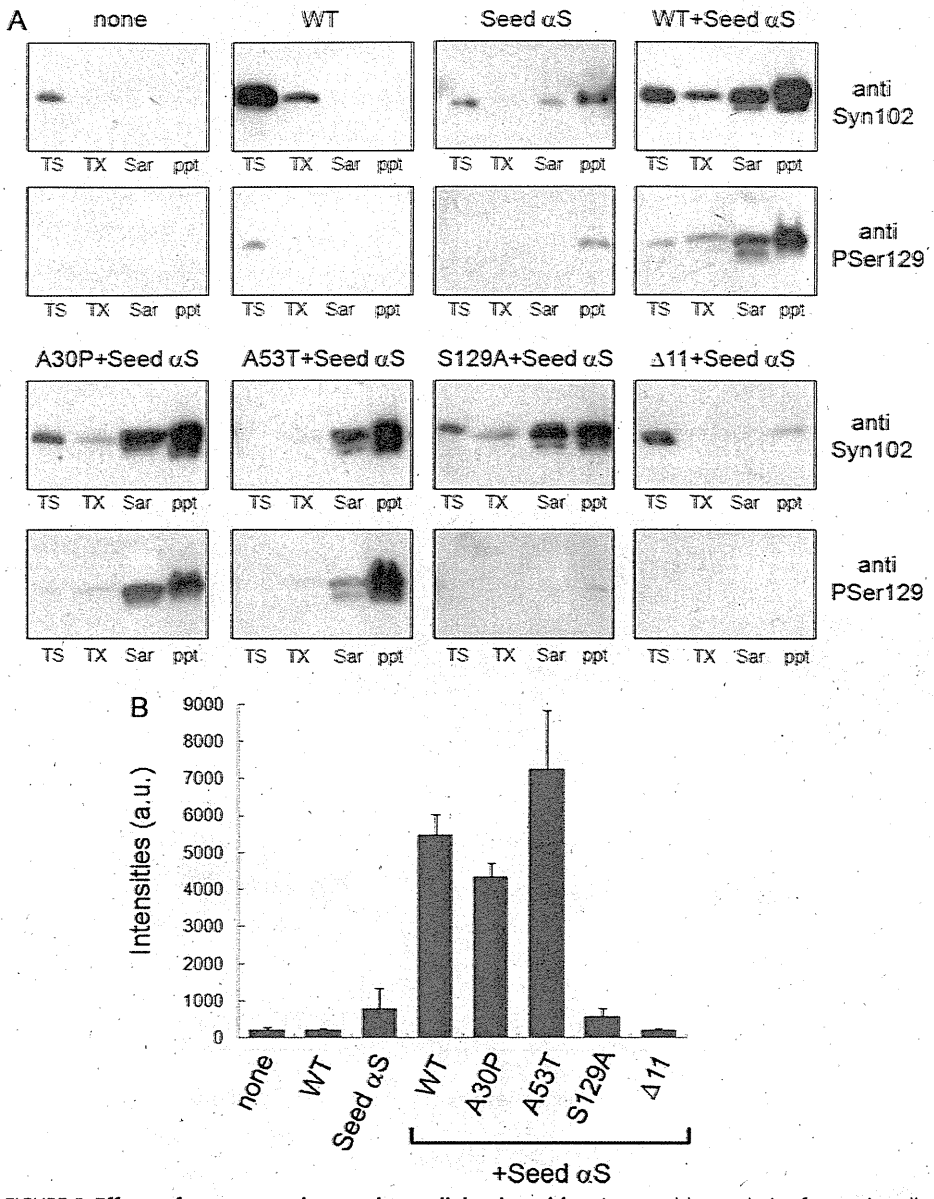

FIGURE 5. **Effects of α-syn mutations on intracellular deposition.** Immunoblot analysis of α-syn in cells transfected with pcDNA3-α-syn alone (*WT*), Seed αS alone (*Seed αS*), both WT and Seed αS (*WT + Seed αS*), and non-treated control cells (*none*). Cells overexpressing familial PD-linked A30P or A53T polymerization-deficient Δ11 mutant α-syn followed by transfection with Seed αS were also analyzed. Proteins were extracted differentially with Tris-HCl (*TS*), Triton-X (*TX*), and Sarkosyl (*Sar*), leaving the pellet (*ppt*), and immunoblotting was done with anti-Syn102 and Ser(P)^{129} (*PSer129*). The Ser(P)^{129}-immunoreactive bands detected in Sarkosyl-soluble and -insoluble fractions from each cell type shown in *A* were quantified (*B*). The results are expressed as means +S.E. (*error bars*) ($n = 3$). a.u., arbitrary unit.

revealed that the levels of Sarkosyl-insoluble α-syn in cells transfected with both α-syn and seeds were reduced by treatment with exifone or gossypetin compared with those in untreated cells (Fig. 7*B*), supporting the notion that these compounds entered the cytoplasm and blocked cell death by suppressing the seed-dependent polymerization of α-syn.

Cellular Models for Nucleation-dependent Polymerization of Tau—Beside α-syn, Tau is another major pathogenic protein that is deposited in degenerating neurons or glial cells in various neurodegenerative diseases, and aggregation of distinct Tau isoforms has been found in different diseases (*i.e.* deposition of three-repeat Tau isoforms in Pick's disease, four-repeat Tau isoforms in progressive supranuclear palsy and corticobasal degeneration, and both three- and four-repeat Tau isoforms in AD). It is unknown why distinct Tau isoforms deposit in different diseases. Thus, we also tried to establish a cellular model of intracellular Tau aggregate formation by transduction of Tau fibril seeds into cultured cells. First, we confirmed that expression of 3R1N or 4R1N by itself induced phosphorylation of Ser^{396}, but no aggregated form was detected in detergent-insoluble fractions (Fig. 8 and supplemental Fig. S5). Next, we tested whether introduced Tau 4R1N or 3R1N fibril seed (Seed 4R1N or 3R1N, respectively) is detectable by immunoblot analysis using anti-T46, anti-HT7, or anti-Ser(P)^{396} antibody. However, we could not detect any band in Triton X-100-insoluble fractions of cells treated with Seed Tau 4R1N or 3R1N in the presence of LA with any of these antibodies (data not shown). It seems likely that the efficiency of introduction of Tau 4R1N and 3R1N fibrils by LA treatment is very low, as compared with that of Seed αS. Then we checked whether treatment with recombinant Tau fibrils causes intracellular Tau aggregate formation in an LA-dependent manner. As shown in supplemental Fig. S5, LA treatment itself did not cause intracellular Tau deposition in cells expressing Tau 4R1N without

FIGURE 4. **α-Syn oligomers were not introduced into cultured cells.** *A* and *B*, α-Syn oligomers were prepared as described under "Experimental Procedures." Oligomeric α-syn protein incubated with (47.8 μg of protein) or without exifone (30 μg of protein) was analyzed by reversed-phase HPLC (Aquapore RP-300 column) (*A*). These samples (0.2 μg of protein of each) were also analyzed by SDS-PAGE and immunoblotted with anti-Syn102 (*B*). *C* and *D*, cells were transfected with empty plasmid (*none*) or pcDNA3-αsyn (*αsyn*) and then treated with or without α-syn oligomer (*Oligomer αS, 5 μg*) or fibrils (*Seed αS, 2 μg*). After incubation for 3 days, cells were harvested, and immunoblot analyses were performed. Proteins differentially extracted from the cells with Tris-HCl (*TS*), Triton X-100 (*TX*), Sarkosyl (*Sar*), and the pellet (ppt) were probed using anti-Syn102 (*C*) and anti-Ser(P)^{129} (*PSer129*) (*D*).

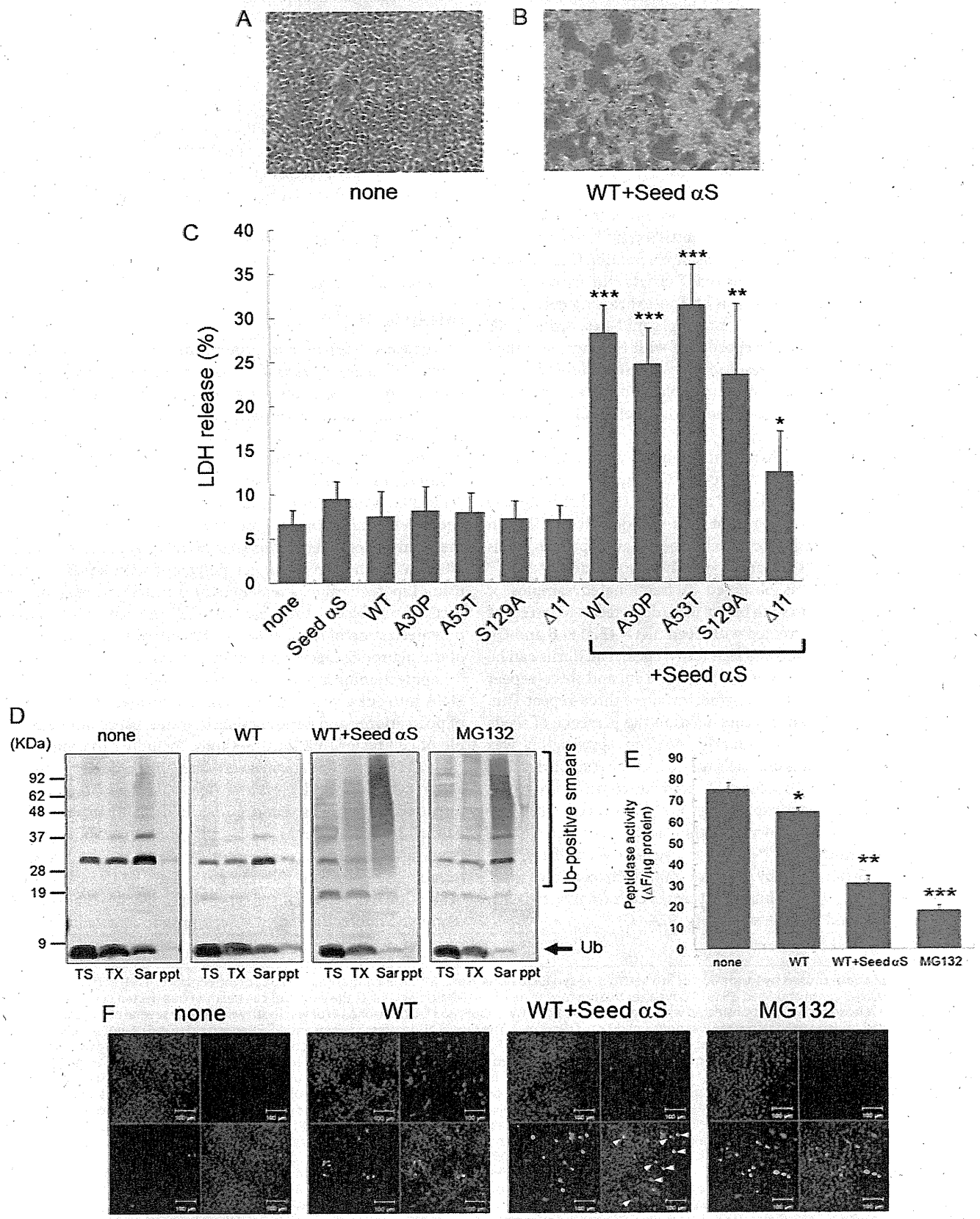

Seed 4R1N. Recombinant Tau 4R1N monomer in the presence of LA did not elicit the formation of intracellular Tau aggregates in these cells. On the other hand, when Seed 4R1N was added to cells expressing Tau 4R1N with LA, aggregated and phosphorylated Tau was detected in Sarkosyl-insoluble fractions by immunoblot analyses of these cell lysates using anti-HT7 or anti-Ser(P)^{396} antibody (supplemental Fig. S5 and Fig. 8). In the case of intracellular Tau 3R1N aggregate formation, the results were similar to those in the experiments using Tau 4R1N described above (data not shown).

Intracellular aggregated four- or three-repeat Tau was also found to be detected with not only anti-Ser(P)^{396} but also anti-AT100 antibody in the Sarkosyl-insoluble fraction (Fig. 8, *B* and *C*). Phosphorylated and deposited Tau was not found in the Triton X-100-insoluble fraction of Tau-expressing cells without Tau seed treatment or mock plasmid-expressing cells treated with Tau seed. In accordance with findings described earlier in this paper, these results suggested that soluble four- or three-repeat Tau expressed from the plasmid was accumulated into intracellular inclusions in the presence of small amounts of Seed 4R1N or 3R1N.

We also found that hyperphosphorylated and aggregated Tau was not detected in three-repeat Tau-expressing cells treated with Seed 4R1N (Fig. 8, *B* and *C*). On the other hand, the aggregated form of three-repeat Tau was detected in Triton X-100-insoluble fractions of three-repeat Tau-expressing cells treated with Seed 3R1N, and hyperphosphorylation at Ser^{396} and Ser^{212}/Thr^{214} was observed in fractionated samples of these cells, whereas no such bands were detected in four-repeat Tau-expressing cells treated with Seed 3R1N (Fig. 8, *B* and *C*). These results clearly showed that four-repeat Tau fibrils can be seeds for polymerization of four-repeat Tau, and three-repeat Tau fibrils can be seeds for polymerization of three-repeat Tau. Tau does not polymerize (cross-seed) in the presence of seeds of a different isoform. Similarly, no Tau aggregation was detected in Tau-expressing cells treated with α-syn fibril seeds (supplemental Fig. S3, *C* and *D*), and no α-syn aggregation was detected in α-syn-expressing cells transduced with Tau fibril seeds (data not shown). Furthermore, we observed anti-AT100 and anti-Ser(P)^{396}-positive Tau 4R1N or 3R1N filaments of ~15-nm width by negative stain electron microscopic analyses of Sarkosyl-insoluble fractions of cells transfected with both Tau plasmid and the seeds (Fig. 9, *A–D*).

Confocal microscopic analyses also showed that GFP-tagged Tau 4R1N (GFP-Tau 4R1N) is aggregated into round inclusions in the presence of Seed 4R1N together with LA (Fig. 8*E*). No inclusion-like structures were found in cells expressing GFP-Tau 4R1N (Fig. 8*D*) or in cells expressing GFP-Tau 4R1N after treatment with Seed 3R1N (data not shown). The ratio of the round aggregates to all GFP-positive transfectants was calculated to be 5.8% ± 0.8602 ($p = 0.0002$ by Student's *t* test against the value of cells expressing GFP-4R1N, $n = 5$). Significant cell death was not observed in cells containing intracellular 3R1N or 4R1N aggregates (data not shown). These results strongly suggest that proteins assemble easily into amyloid fibrils in the presence of amyloid seeds derived from the same protein but not a different protein.

DISCUSSION

Nucleation-dependent protein polymerization occurs in many well characterized physiological processes (*e.g.* microtubule assembly and actin polymerization). It is also the mechanism of amyloid fibril formation in various pathological conditions and has been confirmed to occur *in vitro* for a wide variety of extracellular amyloids, such as Aβ peptides and prion proteins (12, 13) as well as intracellular proteins, such as α-syn and Tau (29, 30, 42). Both extra- and intracellular amyloids have been well studied *in vitro*, but much less is known about the mechanisms of assembly *in vivo*. Here we report a simple and effective method to introduce polymerization seeds into cells using Lipofectamine, a widely used transfection reagent. This method enabled us to evaluate the nucleation-dependent polymerization of α-synuclein and to establish a cellular model of the neurodegeneration seen in Parkinson disease.

Lipofectamine is a reagent widely used for the transfection of DNA into eukaryotic cells through the formation of liposomes of polycationic and neutral lipids in water, based on the principle of cell fusion. Various methods, including microinjection, the calcium phosphate method, the DEAE-dextran method, electroporation, and viral transfer, have been employed to introduce substances that are not normally incorporated into eukaryotic cells under physiological conditions. Microinjection is versatile but is not efficient in experiments involving large numbers of cells, and the traumatic damage to cells hampers evaluation of cytotoxic effects. Here, we have successfully employed lipofection to introduce protein aggregates as seeds

FIGURE 6. **Cell death caused by formation of intracellular α-syn inclusions.** *A* and *B*, phase-contrast microscopy of the control cells (*A*) and cells transfected with both pcDNA3-α-syn and Seed αS (*B*) 3 days after treatment with Seed αS (20× objective). *C*, the extent of cell death of transfected cells was quantified using an LDH release assay. Cells transfected with α-syn plasmid alone (WT, A30P, A53T, S129A, or Δ11) or with both wild-type or several mutants and Seed αS were incubated, and the cell death assay was performed 3 days thereafter. The results are expressed as means +S.E. (*error bars*) ($n = 5$). *, not significant; **, $p < 0.01$; ***, $p < 0.0005$ by Student's *t* test against the value of Seed αS. *D–F*, impairment of proteasome activity caused by intracellular aggregates of α-syn. *D*, immunoblot analysis of proteins sequentially extracted from non-treated cells (*none*) and cells transfected with wild-type α-syn plasmid alone (*WT*) or with both pcDNA3-α-syn and Seed αS (*WT + Seed αS*) and cells treated with 1 μM MG132 for 16 h (MG132) using anti-ubiquitin antibody. An *arrow* indicates monomeric ubiquitin. Polyubiquitinated proteins, reflecting impairment of the proteasome activity, are observed in the Sarkosyl-soluble fraction. *TS*, Tris-soluble; *TX*, 1% Triton X-100-soluble; *Sar*, 1% Sarkosyl-soluble; *ppt*, Sarkosyl-insoluble and SDS-soluble. *E*, peptide hydrolysis activity of proteasome. Cytosol fractions of non-treated control cells (*none*), cells transfected with wild-type α-syn plasmid alone (*WT*) or with WT and Seed αS (*WT + Seed αS*), and cells treated with 20 μM MG132 for 4 h (*MG132*) were prepared and assayed using benzyloxycarbonyl-Leu-Leu-Glu-7-amido-4-methylcoumarin as a substrate. The results are expressed as means +S.E. ($n = 3$). *, $p < 0.05$; **, $p < 0.01$; ***, $p < 0.0005$ by Student's *t* test against the value of none. *F*, proteasome activity in cells having intracellular aggregates of α-syn. SH-SY5Y cells transfected with both GFP-CL1 and WT were treated with Seed αS for 2 days, fixed, and stained with anti-Ser(P)^{129}. In the staining of cells transfected with wild-type α-syn plasmid alone (*WT*), anti-Syn102 was used. As a control, untreated or MG132-treated cells were also stained and analyzed. In untreated control cells, the fluorescence of GFP was poorly detected because GFP-CL1 could be degraded by proteasome in cells. In cells treated with MG132, fluorescence was markedly increased as compared with that in untreated cells because of the inhibition of proteasome activity by MG132. Co-localized images (*arrowheads*) with both increased intensities of GFP (*green*) and the fluorescence of anti-Ser(P)^{129} (*red*) were detected in cells transfected with both WT and Seed αS (*WT + Seed αS*), indicating that the proteasome activity in these cells was inhibited.

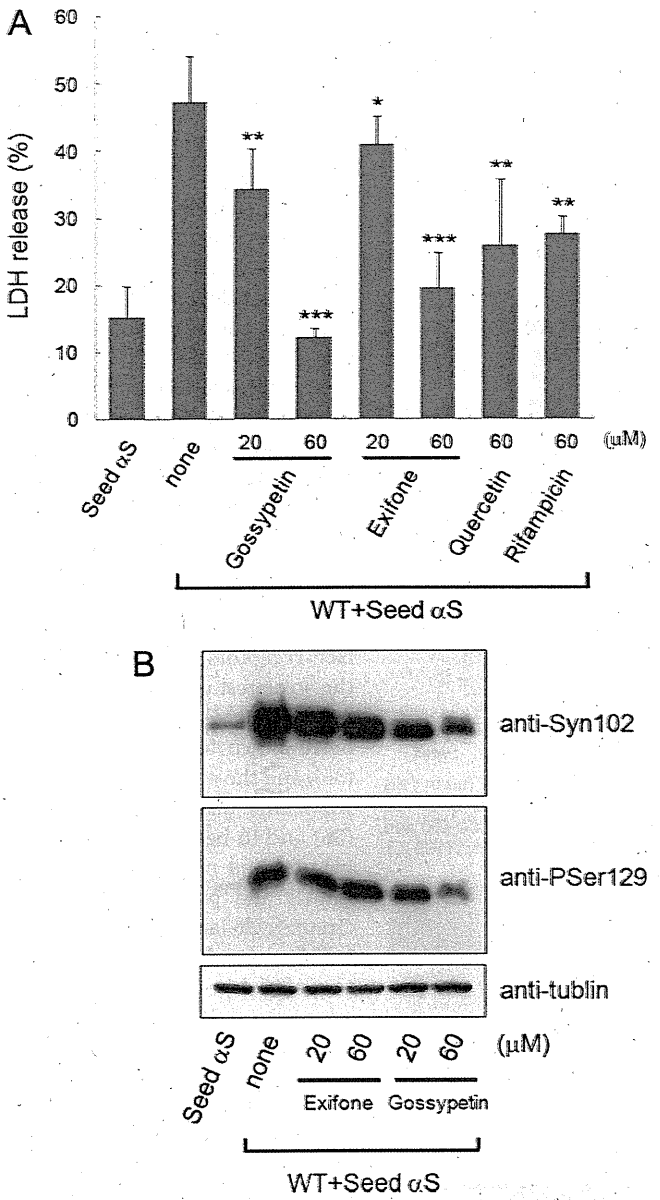

FIGURE 7. **Small molecular inhibitors of amyloid filament formation protect against cell death caused by intracellular α-syn aggregates.** *A*, the cell death of cells transfected with Seed αS and with both α-syn plasmid (*WT*) and Seed αS in the presence or absence of 20 or 60 μM gossypetin, 20 or 60 μM exifone, 60 μM quercetin, or 60 μM rifampicin was quantified by LDH release assay. The results are expressed as means ± S.E. (*error bars*) ($n = 4$). *, not significant; **, $p < 0.05$; ***, $p < 0.0005$ by Student's *t* test against the value of none. *B*, immunoblot analyses of the Sarkosyl-insoluble fraction prepared from cells transfected with Seed αS and with both WT and Seed αS in the absence or presence of exifone or gossypetin, with anti-Syn102 and anti-Ser(P)^{129} (*PSer129*) antibodies. Doubly transfected cells were treated with 20 or 60 μM exifone or gossypetin 2 h after transfection of Seed αS and cultured for 3 days in the presence of polyphenols. Tubulin-α loading controls are also shown.

for amyloid fibril formation (patent pending for the United States (12/086124), the European Union (06834541.2), and Japan (2007-549210)). The reason why Lipofectamine could specifically incorporate Seed αS but not soluble α-syn into cells is unknown. However, one possibility is that aggregated α-syn with an ordered filamentous structure was preferentially bound to Lipofectamine and formed a complex that could be more effectively transported into cells compared with soluble α-syn, which has a random coil structure. In line with this idea, it has been reported that yeast prion fibrils can be introduced into yeast cells (31). Recently, Luk *et al.* (32) have also reported that α-syn monomers and fibrils but not oligomers were introduced into cells by Bioporter, a cationic-liposomal protein transduction reagent.

We confirmed the incorporation of insoluble α-syn seeds into cells by detecting phosphorylation of α-syn, as has been seen in intracellular aggregates of α-syn in various neurodegenerative conditions referred to as synucleinopathies. This suggests that Seed αS introduced into cells is a good target for phosphorylation at Ser^{129}. In contrast to our results, a recent report suggested that α-syn fibrils were not phosphorylated after internalization (32). It is possible that this specific phosphorylation represents an active attempt by cells to maintain the intracellular milieu by sequestering protein species that are harmful to cells. Notably, the phosphorylation of α-syn was dramatically increased when Seed αS was introduced into cells overexpressing soluble α-syn (Fig. 3 and supplemental Figs. S1*D* and S2). The possibility therefore arises that widespread propagation of hyperphosphorylation of α-syn throughout the cytoplasm reflects the activation of a certain kinase(s) associated with conversion of soluble α-syn into the fibrillar form in the presence of Seed αS. However, further investigation is needed to elucidate the importance of phosphorylation for protein aggregation.

The significance of intracellular and extracellular protein aggregates in neurodegeneration is still a matter of debate. The present results clearly show that nucleation-dependent polymerization of amyloid-like proteins is closely related to neuronal degeneration leading to cell death. According to the seeding theory, amyloid fibrils grow rapidly, without a time lag, when seeds are exposed to an amount of amyloidogenic soluble protein that exceeds the critical concentration. Our experiments with seed-transfected SH-SY5Y cells overexpressing α-syn clearly demonstrated that this is the case in the intracellular environment. We have unequivocally demonstrated that nucleation-dependent polymerization of amyloid-like fibrils can occur inside cells, and the intracellular filament formation elicits a variety of cellular reactions, including hyperphosphorylation and compromise of the ubiquitin proteasome system. We also showed that α-syn oligomers were not introduced into cells by LA and did not function as seeds for α-syn aggregate formation in cultured cells. It has been speculated that protein fibrils, not oligomers, are spread or transmitted in recently reported *in vivo* models (25, 33).

Our study also revealed that intracellular protein aggregation is highly dependent on the species of protein fibril seeds. This important finding may explain why only certain Tau isoforms are deposited in several tauopathies, including Pick disease, progressive supranuclear palsy, and corticobasal degeneration. In this study, α-syn fibrils were shown to be unable to seed intracellular Tau aggregation, which is consistent with neuropathological reports that deposited α-syn is not markedly co-localized with Tau aggregates. Our observations strongly support a seed-dependent mechanism for the formation of the intracellular protein aggregates.

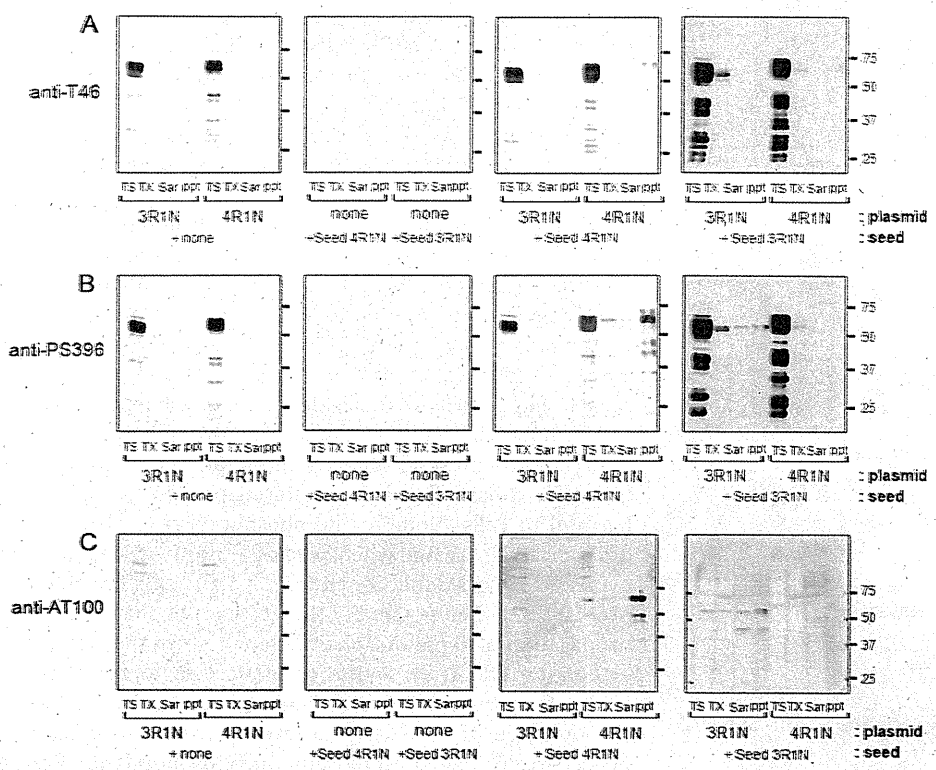

FIGURE 8. **Immunoblot analyses of intracellular Tau aggregates.** *A–C*, immunoblot analysis of Tau in cells treated with Tau fibrils alone (Seed 3R1N or Seed 4R1N), pcDNA3-Tau alone (3R1N or 4R1N), or both Seed Tau and pcDNA3-Tau. Tau proteins differentially extracted from the cells with Tris-HCl (*TS*), Triton X-100 (*TX*) and Sarkosyl (*Sar*), and the pellet (*ppt*) were probed with anti-T46 (*A*), anti-Ser(P)^{396} (*PS396*) (*B*), and anti-AT100 (*C*).

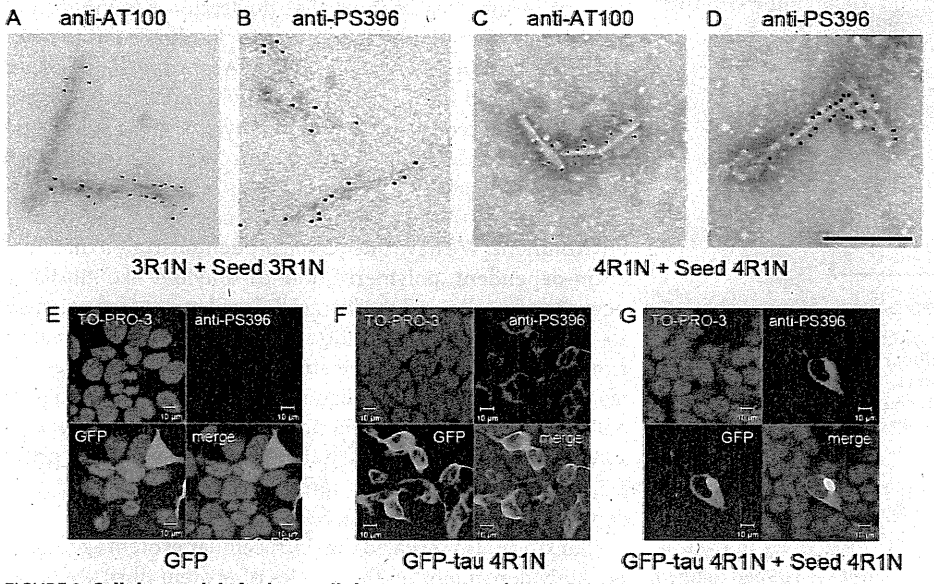

FIGURE 9. **Cellular models for intracellular Tau aggregation.** *A–D*, immunoelectron microscopy of Tau filaments extracted from transfected cells. SH-SY5Y cells were transfected with both pcDNA3-Tau 3R1N and Seed 3R1N (*A* and *B*) or pcDNA3-Tau 4R1N and Seed 4R1N (*C* and *D*). The Sarkosyl-insoluble fraction was prepared from the cells, and the filaments were immunolabeled with anti-AT100 (*A* and *C*) or anti-Ser(P)^{396} (*PS396*) (*B* and *D*) antibody. *Scale bar*, 200 nm. *E–G*, confocal laser microscopic analyses of SH-SY5Y cells transfected with pEGFP empty vector (*E*), pEGFP-Tau 4R1N (*F*), and cells transfected with both pEGFP-Tau 4R1N and Seed 4R1N (*G*), immunostained with anti-Ser(P)^{396} (*red*), and counterstained with TO-PRO-3 (*blue*). *Scale bars*, 10 μm.

shed from one cell may easily be propagated to others (*e.g.* neurons or glial cells) under pathological conditions (*e.g.* alteration in membrane permeability due to aging or virus infection, impairment of membrane function as a result of physical interaction with extracellular amyloid deposits, or abnormal membrane depolarization) that favor intracellular deposition of protein fibrils.

It remains to be clarified whether the incorporation of amyloid seeds into neurons or glial cells, as shown in this study, also occurs *in vivo*. However, some observations in AD or in transgenic animals support this possibility; apolipoprotein E (apoE) is involved in lipoprotein particle uptake mediated by cell surface receptors, and the E4 allele is the strongest genetic risk factor for AD. The apoE polypeptide has also been shown to bind Aβ (34), Tau (35), and the non-Aβ component of Alzheimer disease region of α-syn (36) and to be localized in amyloid plaques and neurofibrillary tangles in AD and prion plaques (37) in Creutzfeldt-Jakob disease. ApoE and low density lipoprotein receptor-related protein facilitate intraneuronal Aβ42 accumulation in transgenic mice (38). Furthermore, activation of both endocytic uptake and recycling of these proteins at a preclinical stage has been reported in sporadic AD and Down syndrome (39). Thus, it is strongly suggested that extracellular amyloid may be taken up into neurons by apoE and lipoprotein receptor-related protein-mediated endocytosis. Therefore, intracellular amyloid seeds composed of α-syn or Tau may also be incorporated into neurons by similar mechanisms when these seeds are released to the extracellular space after neuronal death.

It is well established that Tau protein starts to accumulate in the entorhinal region and spreads to the neocortices, closely correlating with the progression of AD (40). Similarly, accumulation of phosphorylated α-syn has been shown to start in vulnerable regions (*i.e.* limbic cortices) and to spread to the neocortices in PD or DLB. However, the mechanism of propagation of abnormal

Importantly, we showed that seed α-syn or Tau, an insoluble aggregate prepared from α-syn or Tau filaments, is effectively incorporated into cells by lipofection. This, in turn, suggests that high molecular weight protein aggregates or amyloid seeds

protein deposition remains unknown. This study strongly supports a seed-dependent mechanism for the formation of the intracellular protein aggregates. In the context of our propagation hypothesis, it will be crucial to inhibit not only the production of intracellular amyloid seeds but also their spread into the extracellular space. Vaccination against the intracellular amyloid proteins, such as α-syn (41) or Tau may be an effective approach, together with inhibition of intracellular amyloid filament formation by small molecular inhibitors, for the therapy of these diseases.

Acknowledgments—We thank Yoko Shimomura, Masami Masuda, and Ayaho Dan for technical assistance with immunoelectron microscopy and the preparation of recombinant Tau protein. We also thank Michel Goedert for helpful comments on the manuscript.

REFERENCES

1. Chiti, F., and Dobson, C. M. (2006) *Annu. Rev. Biochem.* **75,** 333–366
2. Goedert, M., Spillantini, M. G., and Davies, S. W. (1998) *Curr. Opin Neurobiol.* **8,** 619–632
3. Prusiner, S. B. (2001) *N. Engl. J. Med.* **344,** 1516–1526
4. Soto, C., Estrada, L., and Castilla, J. (2006) *Trends Biochem. Sci.* **31,** 150–155
5. Fujiwara, H., Hasegawa, M., Dohmae, N., Kawashima, A., Masliah, E., Goldberg, M. S., Shen, J., Takio, K., and Iwatsubo, T. (2002) *Nat. Cell Biol.* **4,** 160–164
6. Kirschner, D. A., Inouye, H., Duffy, L. K., Sinclair, A., Lind, M., and Selkoe, D. J. (1987) *Proc. Natl. Acad. Sci. U.S.A.* **84,** 6953–6957
7. Eanes, E. D., and Glenner, G. G. (1968) *J. Histochem. Cytochem.* **16,** 673–677
8. Nguyen, J. T., Inouye, H., Baldwin, M. A., Fletterick, R. J., Cohen, F. E., Prusiner, S. B., and Kirschner, D. A. (1995) *J. Mol. Biol.* **252,** 412–422
9. Serpell, L. C., Berriman, J., Jakes, R., Goedert, M., and Crowther, R. A. (2000) *Proc. Natl. Acad. Sci. U.S.A.* **97,** 4897–4902
10. Berriman, J., Serpell, L. C., Oberg, K. A., Fink, A. L., Goedert, M., and Crowther, R. A. (2003) *Proc. Natl. Acad. Sci. U.S.A.* **100,** 9034–9038
11. Perutz, M. F. (1999) *Trends Biochem. Sci.* **24,** 58–63
12. Harper, J. D., and Lansbury, P. T., Jr. (1997) *Annu. Rev. Biochem.* **66,** 385–407
13. Jarrett, J. T., and Lansbury, P. T., Jr. (1993) *Cell* **73,** 1055–1058
14. Jakes, R., Spillantini, M. G., and Goedert, M. (1994) *FEBS Lett.* **345,** 27–32
15. Nonaka, T., Iwatsubo, T., and Hasegawa, M. (2005) *Biochemistry* **44,** 361–368
16. Aoyagi, H., Hasegawa, M., and Tamaoka, A. (2007) *J. Biol. Chem.* **282,** 20309–20318
17. Taniguchi, S., Suzuki, N., Masuda, M., Hisanaga, S., Iwatsubo, T., Goedert, M., and Hasegawa, M. (2005) *J. Biol. Chem.* **280,** 7614–7623
18. Nonaka, T., Kametani, F., Arai, T., Akiyama, H., and Hasegawa, M. (2009) *Hum. Mol. Genet.* **18,** 3353–3364
19. Nonaka, T., and Hasegawa, M. (2009) *Biochemistry* **48,** 8014–8022
20. Sung, J. Y., Kim, J., Paik, S. R., Park, J. H., Ahn, Y. S., and Chung, K. C. (2001) *J. Biol. Chem.* **276,** 27441–27448
21. Spillantini, M. G., Crowther, R. A., Jakes, R., Hasegawa, M., and Goedert, M. (1998) *Proc. Natl. Acad. Sci. U.S.A.* **95,** 6469–6473
22. Conway, K. A., Rochet, J. C., Bieganski, R. M., and Lansbury, P. T., Jr. (2001) *Science* **294,** 1346–1349
23. Masuda, M., Suzuki, N., Taniguchi, S., Oikawa, T., Nonaka, T., Iwatsubo, T., Hisanaga, S., Goedert, M., and Hasegawa, M. (2006) *Biochemistry* **45,** 6085–6094
24. Giasson, B. I., Murray, I. V., Trojanowski, J. Q., and Lee, V. M. (2001) *J. Biol. Chem.* **276,** 2380–2386
25. Desplats, P., Lee, H. J., Bae, E. J., Patrick, C., Rockenstein, E., Crews, L., Spencer, B., Masliah, E., and Lee, S. J. (2009) *Proc. Natl. Acad. Sci. U.S.A.* **106,** 13010–13015
26. Hasegawa, M., Fujiwara, H., Nonaka, T., Wakabayashi, K., Takahashi, H., Lee, V. M., Trojanowski, J. Q., Mann, D., and Iwatsubo, T. (2002) *J. Biol. Chem.* **277,** 49071–49076
27. Bence, N. F., Sampat, R. M., and Kopito, R. R. (2001) *Science* **292,** 1552–1555
28. Gilon, T., Chomsky, O., and Kulka, R. G. (1998) *EMBO J.* **17,** 2759–2766
29. Friedhoff, P., von Bergen, M., Mandelkow, E. M., Davies, P., and Mandelkow, E. (1998) *Proc. Natl. Acad. Sci. U.S.A.* **95,** 15712–15717
30. Wood, S. J., Wypych, J., Steavenson, S., Louis, J. C., Citron, M., and Biere, A. L. (1999) *J. Biol. Chem.* **274,** 19509–19512
31. Tanaka, M., Chien, P., Yonekura, K., and Weissman, J. S. (2005) *Cell* **121,** 49–62
32. Luk, K. C., Song, C., O'Brien, P., Stieber, A., Branch, J. R., Brunden, K. R., Trojanowski, J. Q., and Lee, V. M. (2009) *Proc. Natl. Acad. Sci. U.S.A.* **106,** 20051–20056
33. Clavaguera, F., Bolmont, T., Crowther, R. A., Abramowski, D., Frank, S., Probst, A., Fraser, G., Stalder, A. K., Beibel, M., Staufenbiel, M., Jucker, M., Goedert, M., and Tolnay, M. (2009) *Nat. Cell Biol.* **11,** 909–913
34. Strittmatter, W. J., Saunders, A. M., Schmechel, D., Pericak-Vance, M., Enghild, J., Salvesen, G. S., and Roses, A. D. (1993) *Proc. Natl. Acad. Sci. U.S.A.* **90,** 1977–1981
35. Strittmatter, W. J., Saunders, A. M., Goedert, M., Weisgraber, K. H., Dong, L. M., Jakes, R., Huang, D. Y., Pericak-Vance, M., Schmechel, D., and Roses, A. D. (1994) *Proc. Natl. Acad. Sci. U.S.A.* **91,** 11183–11186
36. Olesen, O. F., Mikkelsen, J. D., Gerdes, C., and Jensen, P. H. (1997) *Brain Res. Mol. Brain Res.* **44,** 105–112
37. Namba, Y., Tomonaga, M., Kawasaki, H., Otomo, E., and Ikeda, K. (1991) *Brain Res.* **541,** 163–166
38. Zerbinatti, C. V., Wahrle, S. E., Kim, H., Cam, J. A., Bales, K., Paul, S. M., Holtzman, D. M., and Bu, G. (2006) *J. Biol. Chem.* **281,** 36180–36186
39. Cataldo, A. M., Peterhoff, C. M., Troncoso, J. C., Gomez-Isla, T., Hyman, B. T., and Nixon, R. A. (2000) *Am. J. Pathol.* **157,** 277–286
40. Braak, H., and Braak, E. (1991) *Acta Neuropathol.* **82,** 239–259
41. Masliah, E., Rockenstein, E., Adame, A., Alford, M., Crews, L., Hashimoto, M., Seubert, P., Lee, M., Goldstein, J., Chilcote, T., Games, D., and Schenk, D. (2005) *Neuron* **46,** 857–868
42. Yonetani, M., Nonaka, T., Masuda, M., Inukai, Y., Oikawa, T., Hisanaga, S. I., and Hasegawa, M. (2009) *J. Biol. Chem.* **284,** 7940–7950

Supplemental data

Seeded aggregation and toxicity of α-synuclein and tau: cellular models of neurodegenerative diseases

Takashi Nonaka, Sayuri T. Watanabe, Takeshi Iwatsubo, Masato Hasegawa

Supplemental figure legends

Figure S1. Time-course observation of cells transduced with Seed αS.
(A-B) Electron microscopic analyses of Seed αS used in this study with (B) or without (A) sonication before use. Scale bars, 200 nm.
(C) Confocal microscopic images of SH-SY5Y cells 1 day and 3 days after treatment with Seed-HA in the presence or absence of LA. Cells were stained with anti-HA (red), anti-PSer129 (green) and TO-PRO-3 (blue). Scale bars, 50 μm.
(D) Confocal microscopic images of SH-SY5Y cells transfected with or without pcDNA3-αsyn (WT) 1 day and 3 days after treatment with or without Seed-HA. Cells were stained with anti-HA (red), anti-PSer129 (green) and TO-PRO-3 (blue). Scale bars, 50 μm.

Figure S2. Intracellular α-syn aggregate formation is dependent on the amount of α-syn seeds.
Cells were transfected with pcDNA3-αsyn (αsyn) and then transduced with different amounts of Seed-HA. After incubation for 3 days, cells were harvested and immunoblot analyses of the lysates was performed. α-Syn differentially extracted from the cells with Tris-HCl (TS), Triton X-100 (TX), and Sarkosyl (Sar), and the pellet (ppt), were probed using anti-HA (A) and anti-PSer129 (B). Immunoreactivity of phosphorylated α-syn in the TX-insoluble fraction was quantified using anti-PSer129. The results are shown in (C).

Figure S3. α-Syn fibrils seed intracellular aggregate formation of plasmid-derived α-syn, but not tau.
Cells were transfected with empty plasmid (none), pcDNA3-αsyn (αsyn) or pcDNA3-tau 3R1N (3R1N) and then treated with Seed-HA. After incubation for 3 days, cells were harvested and immunoblot analyses were performed. Proteins differentially extracted from the cells with Tris-HCl (TS), Triton X-100 (TX), and Sarkosyl (Sar), and the pellet (ppt), were probed using

anti-HA (A), anti-PSer129 (B), anti-T46 (C) and anti-PS396 (D).

Figure S4. Apoptosis is not induced in cells harboring intracellular α-syn aggregates.
(A) TUNEL staining of cells treated without (none) or with 1 μM staurosporine (stsp) for 8 hr and cells transfected with or without pcDNA3-αsyn (WT) 3 days after treatment with or without Seed αS. Cells were stained with TUNEL reagent (green), anti-PSer129 (red) and TO-PRO-3 (blue). Scale bars, 100 μm.
(B) The measurement of caspase-3 activity in cultured cells. Cells were transfected with empty plasmid (none) or pcDNA3-αsyn (WT) and then treated with or without Seed αS. After incubation for 3 days, cells were harvested and caspase-3 activity in the lysates was measured using Ac-DEVD-MCA as a substrate. Cell lysate treated with stsp was used as a positive control.

Fig. S5. Introduction of tau 4R1N monomer and fibril seed by Lipofectamine.

Purified recombinant tau (4R1N monomer; 2 μg) and filaments (Seed 4R1N, 2 μg) were sonicated and then incubated with Lipofectamine (LA). The protein-LA complexes were dispersed in opti-MEM and added to SH-SY5Y cells expressing pcDNA3-tau 4R1N. After 48 hr of culture, the cells were collected in the presence of 0.25% trypsin, and tau proteins were differentially extracted from the cells with Tris-HCl (TS), Triton X-100 (TX) and Sarkosyl (Sar), and the pellet (ppt), were probed with anti-T46 (upper), anti-HT7 (middle) and anti-PS396 (lower).

Fig. S1 Nonaka et al

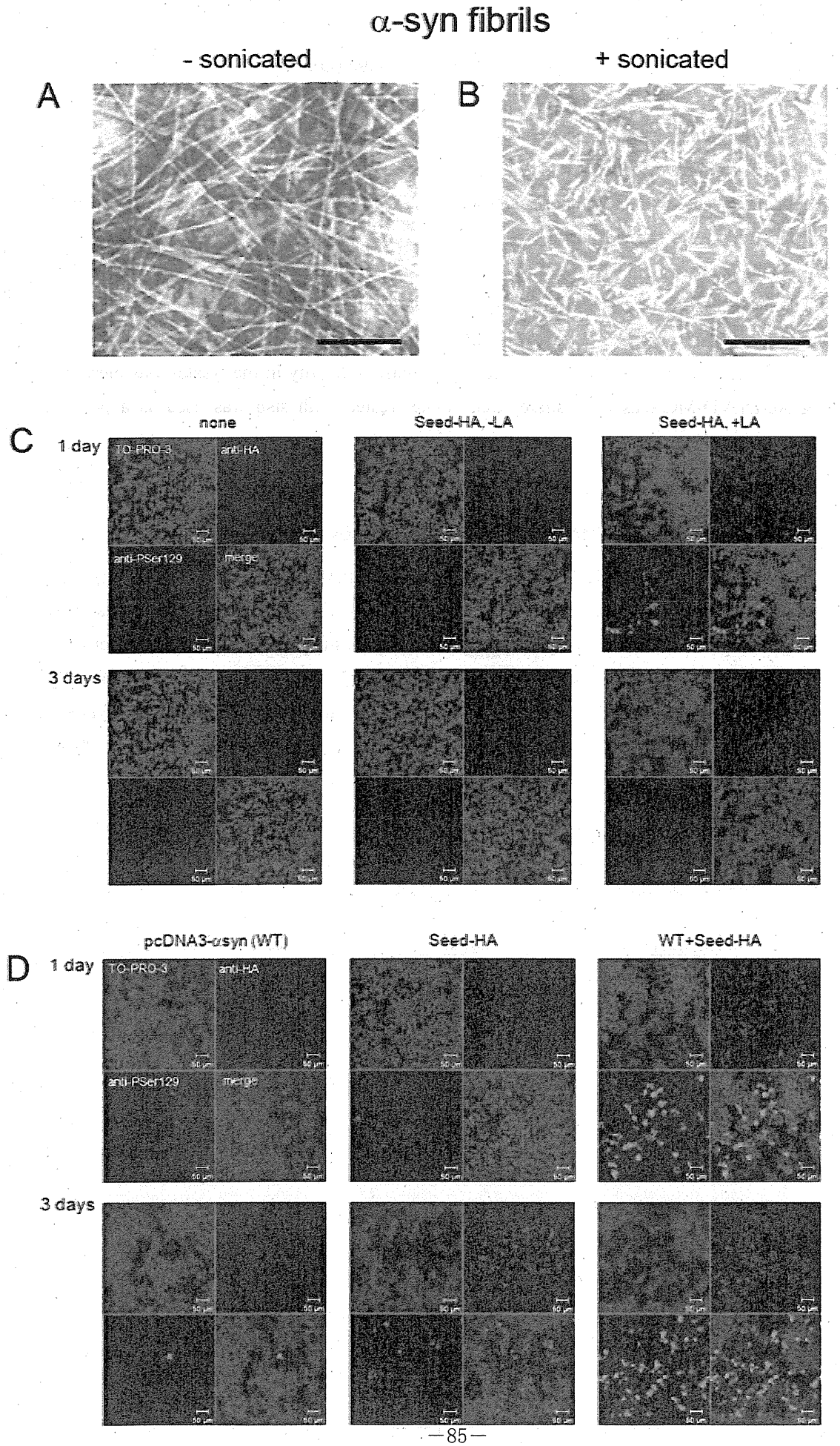

Fig. S2 Nonaka et al

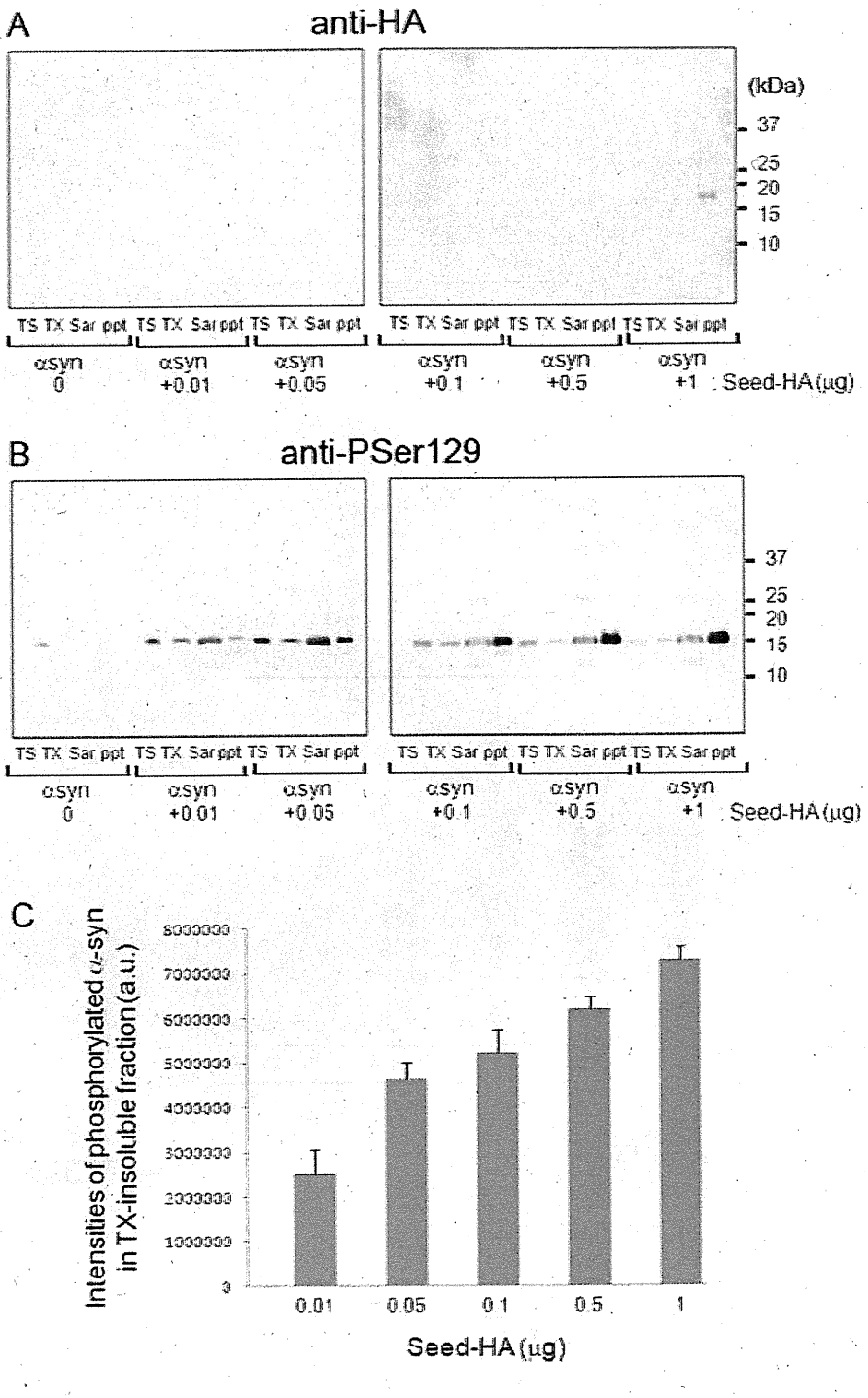

Fig. S3 Nonaka et al

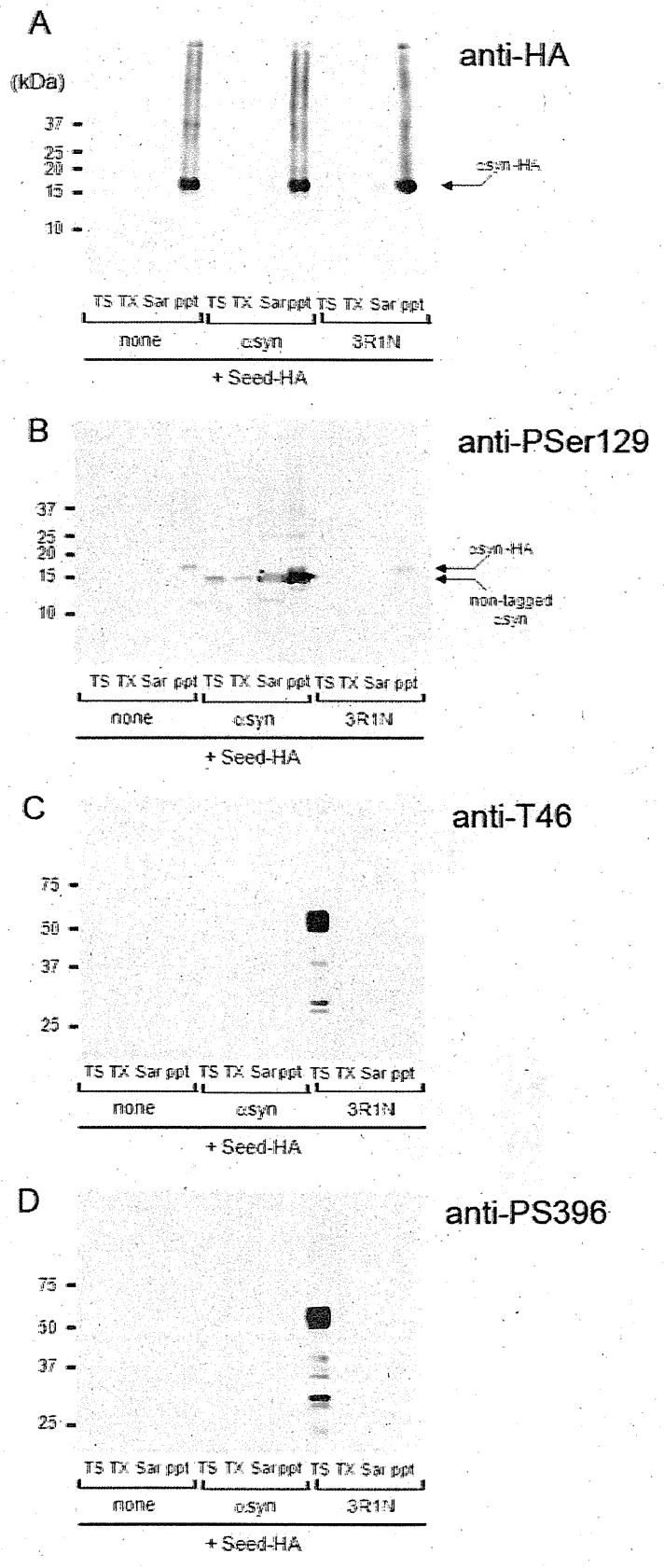

Fig. S4 Nonaka et al

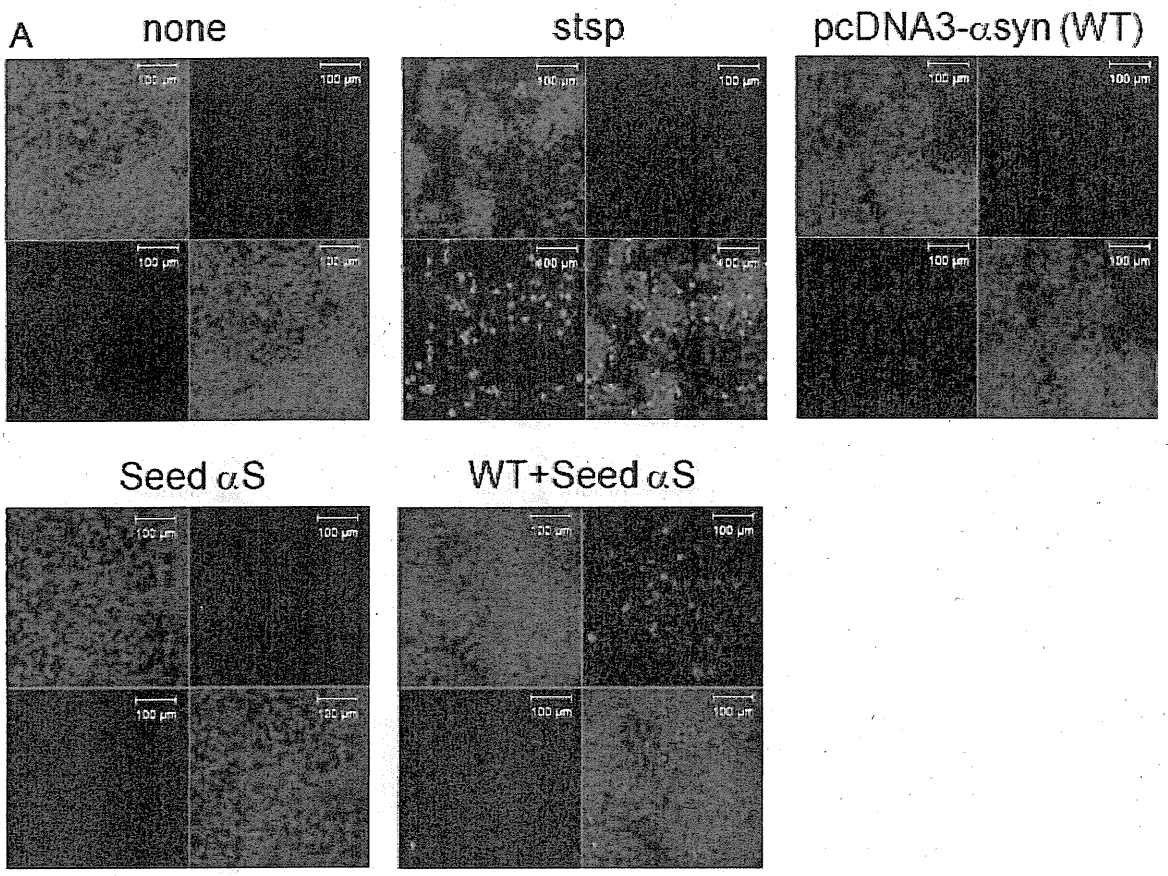

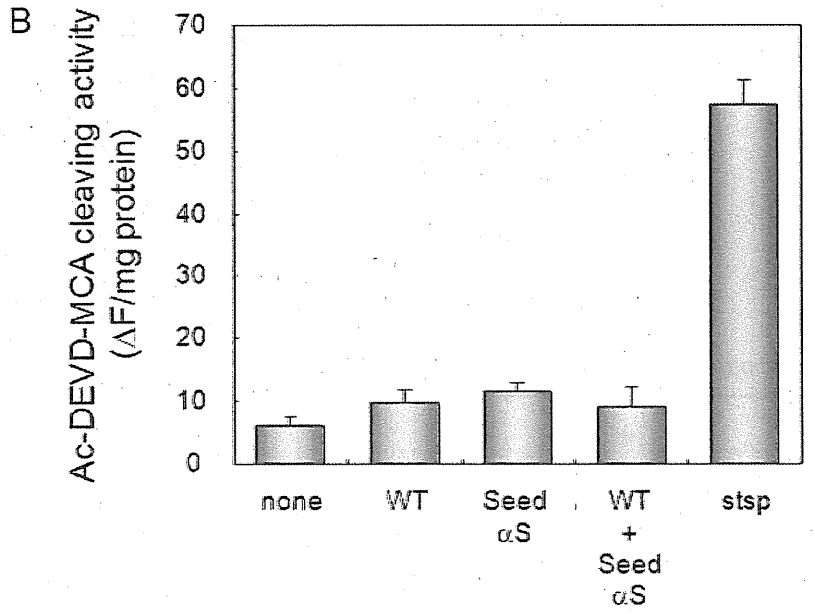

Fig. S5 Nonaka et al

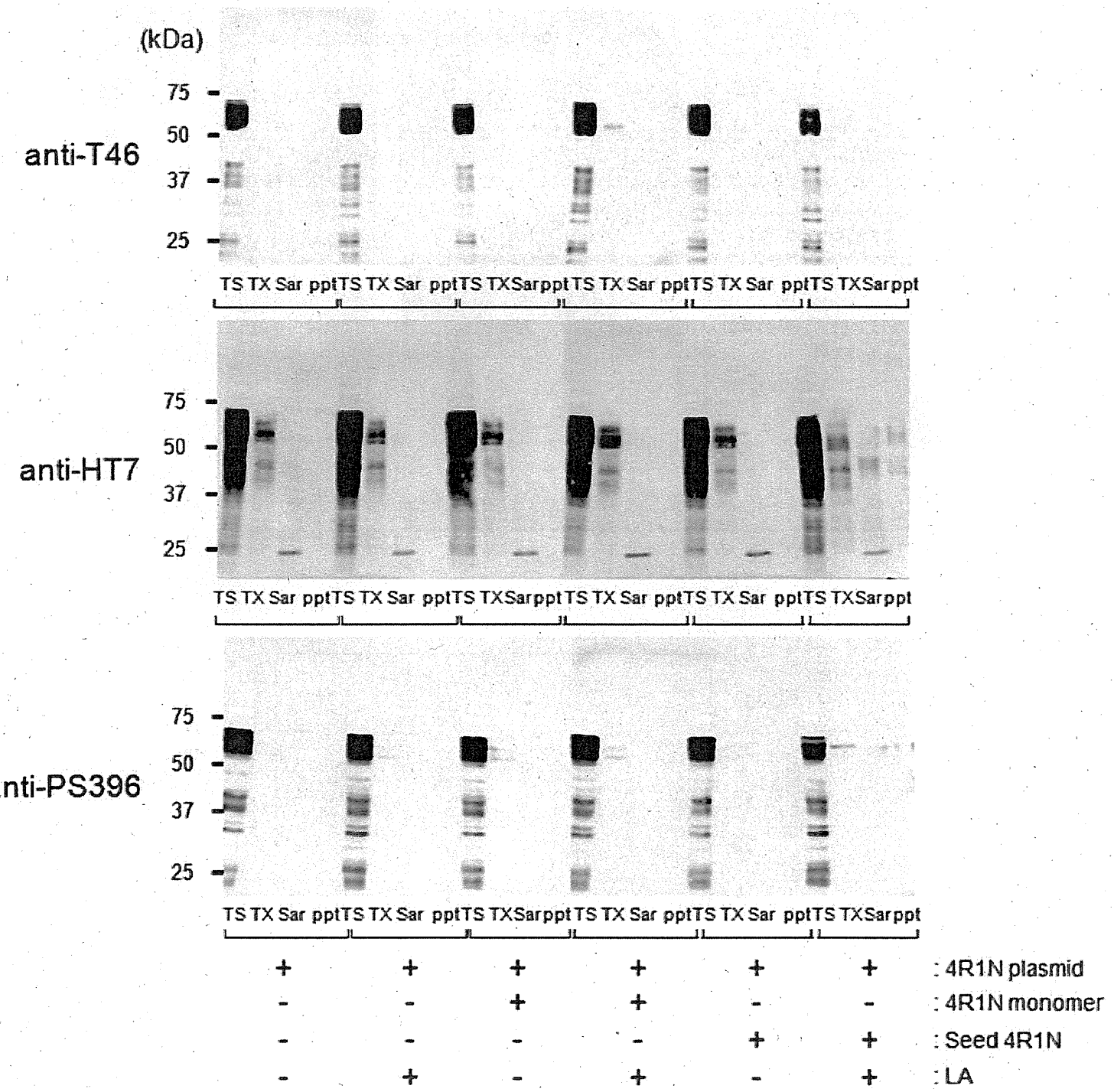

PSYCHOGERIATRICS
The Official Journal of the Japanese Psychogeriatric Society

doi:10.1111/j.1479-8301.2010.00318.x PSYCHOGERIATRICS 2010; 10: 69–76

ORIGINAL ARTICLE

Argyrophilic grain disease with delusions and hallucinations: a pathological study

Toshiyasu ASAOKA,[1] Kuniaki TSUCHIYA,[2] Hiroshige FUJISHIRO,[3,4] Tetsuaki ARAI,[4] Masato HASEGAWA,[5] Haruhiko AKIYAMA,[4] Eizo ISEKI,[3] Tatsuro ODA,[1] Mitsumoto ONAYA[1] and Itaru TOMINAGA[1]

[1]Department of Psychiatry, Shimousa Psychiatric Medical Center, Midori-ku, Chiba, [2]Department of Laboratory Medicine and Pathology, Tokyo Metropolitan Matsuzawa Hospital, Setagaya-ku, [3]PET/CT Dementia Research Center, Juntendo Tokyo Koto Geriatric Medical Center, Juntendo University School of Medicine, Koto-ku, [4]Department of Psychogeriatrics, and [5]Department of Molecular Neurobiology, Tokyo Institute of Psychiatry, Setagaya-ku, Tokyo, Japan

Correspondence: Dr Hiroshige Fujishiro MD, PhD, PET/CT Dementia Research Center, Juntendo Tokyo Koto Geriatric Medical Center, Juntendo University School of Medicine, 3-3-20 Shinsuna, Koto-ku, Tokyo 136-0075, Japan. Email: fujishiro17@hotmail.co.jp

Received 6 October 2009; accepted 22 January 2010.

Key words: *AGD, autopsy, dementia, phosphorylation, psychiatric symptom, tau, TDP-43.*

Abstract

No clear clinical syndrome for argyrophilic grain disease (AGD) has yet been identified. Previous studies have documented its clinical features, namely, personality changes characterized by emotional disorder involving aggression or ill temper and relatively well-preserved cognitive function, but the clinical manifestations of delusions and hallucinations as they appear in AGD have not been thoroughly described. Here, we report on a 72-year-old Japanese AGD patient who showed psychiatric symptoms, memory impairment and emotional change. He perceived and described a person who was not present and tried to grasp things on the floor though nothing was there. He also insisted that somebody was watching him and consequently always kept his curtains closed. These psychiatric symptoms were observed at an early stage in the patient's disease course. Serial neuroradiological examination showed progressive atrophy of the bilateral temporal lobes. The patient died at 79 years-of-age. Microscopic neuropathological examination showed transactivation responsive region (TAR)-DNA-binding protein of 43 kDa (TDP-43) positive structures in addition to widespread argyrophilic grains and coiled bodies. According to recent recommendations for pathological diagnosis, this case corresponds to AGD with limbic TDP-43 pathology. This case shows that patients with AGD that is eventually confirmed through autopsy can present with delusions and hallucinations early in the course of their disease. The clinical significance of TDP-43 pathology in the brains of patients with AGD remains uncertain.

INTRODUCTION

Argyrophilic grain disease (AGD) was first described by Braak and Braak in the brains of patients with adult-onset dementia.[1] AGD is neuropathologically characterized by the presence of small spindle- or comma-shaped silver stain-positive structures, so-called argyrophilic grains, in the neuropil in the limbic area, which includes the hippocampus, the entorhinal and transentorhinal cortices and the cingulate cortex.[1–3] Recently, Togo *et al.* classified AGD as 4-repeat tauopathy, such as progressive supranuclear palsy (PSP) and corticobasal degeneration (CBD), based on the morphological, biochemical and genetic analyses.[4,5] Previous studies have documented its clinical features, namely, personality changes characterized by emotional disorder involving aggression or ill temper and relatively well-preserved cognitive function, but the clinical manifestations of delusions and hallucinations as they appear in AGD have not been thoroughly described.[6,7] In the present study, we report the clinical course of an AGD case showing delusions and hallucinations with serial radiological examinations. On neuropathological evaluation, in addition to argyrophilic grains confirmed by modified

Gallyas–Braak staining, detailed immunostaining showed transactivation responsive region (TAR)-DNA-binding protein of 43 kDa (TDP-43) positive structures. The purpose of the present study was to review clinical, radiological and pathological features of this AGD case with TDP-43 immunoreactive pathology, including double-labeling immunofluorescence for phosphorylated tau and phosphorylated TDP-43.

CASE REPORT

An elderly 79-year-old man had progressive cognitive impairment. He had no family history of dementia or neurological disease. His past medical history included colon cancer, ileus and chronic bronchitis. While he suffered from colon cancer at 72 years-of-age, he presented with delirium after operation. After discharge, he developed memory impairment and fell frequently. He became restless and irritated in the evenings, and requested his wife follow his orders. He perceived and described a person who was not present and tried to grasp things on the floor though nothing was there, suggesting hallucinations. He also insisted that somebody was watching him and consequently always kept his curtains closed. These psychiatric symptoms were observed at an early stage in the patient's disease course. At 74 years of age his symptoms were getting worse, and the patient was admitted to a care unit for dementia in a psychiatric hospital because of his wife's severe burden of taking care of him. At admission, his Mini-Mental State Examination score was 22; orientation of place, 3/5; serial 7, 3/5; remote memory, 0/3; and repetition, 0/1. Computed tomography (CT) of his head showed prominent bilateral inferior ventricle enlargement with slight asymmetry and mild cortical atrophy (Fig. 1a). After hospitalization, he wanted to go home with complaints of inappropriate hospitalization and was uncooperative with medical staff. He was discharged to a health services facility for the elderly several times, but needed to be admitted to a care unit for dementia again because of troubles with other patients, including fighting and stealing. At hospitalization, he lost his temper easily and his social interpersonal conduct declined. When the nurse revealed his stealing to other patients, he apologized and returned the items to them, showing preserved insight into his behavior. He could tell the staff at his bedside his need to urinate a few months before his death. Subsequent head CT showed progressive degeneration of temporal lobes, with relative preservation of the other cortical lobes (Fig. 1b,c). Coronal magnetic resonance imaging (MRI) showed severe temporal atrophy: slightly asymmetric and highly marked atrophy in the anterior mediotemporal lobe 7 months before death (Fig. 2). He died from pneumonia at 79 years-of-age. His clinical duration of dementia was approximately 8 years. Written informed consent from his family was provided before an autopsy was carried out.

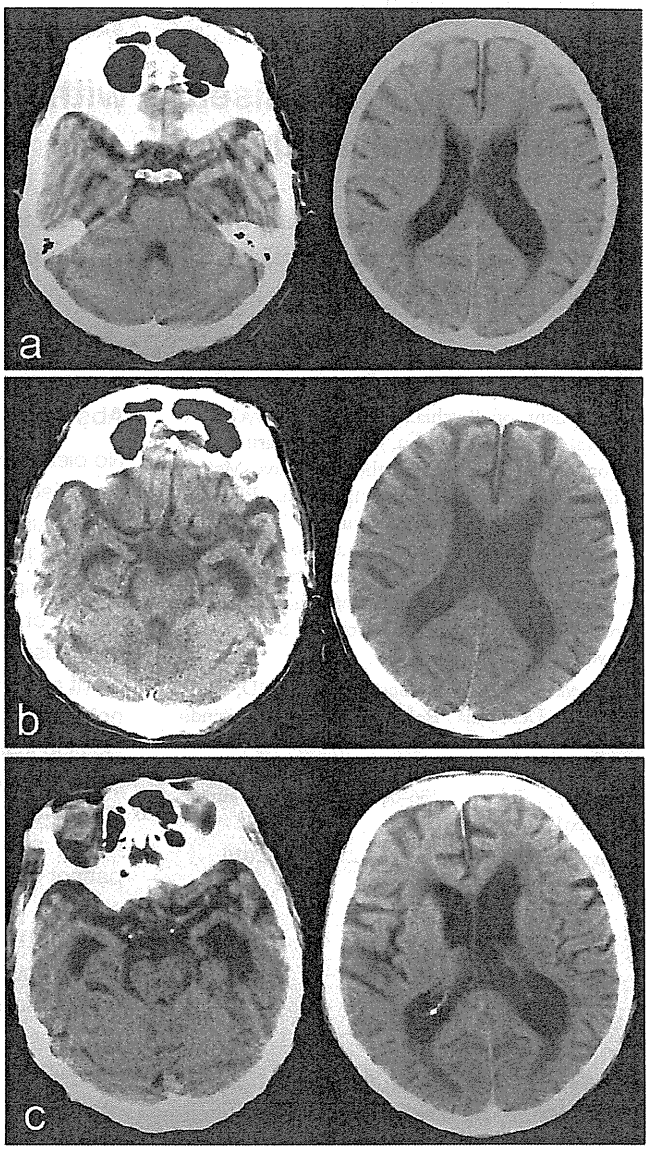

Figure 1 Computed tomography scans showing progressive enlargement of bilateral inferior ventricles. The temporal lobe showed progressive atrophy, whereas other cortical regions were relatively preserved in the course of the disease. Scans were taken (a) 3 years, (b) 5 years, and (c) 8 years (2 months before death) after the disease onset.